Acta Pharmaceutica Sinica B 2025;15(11):5803−5816

Chinese Pharmaceutical Association
Institute of Materia Medica, Chinese Academy of Medical Sciences

Acta Pharmaceutica Sinica B

www.elsevier.com/locate/apsb
www.sciencedirect.com

ORIGINAL ARTICLE

CRTAC1 derived from senescent FLSs induces chondrocyte mitochondrial dysfunction *via* modulating NRF2/SIRT3 axis in osteoarthritis progression

Xiang Chen[a,b,c,†], Wang Gong[a,b,c,†], Pan Zhang[a,b,c], Chengzhi Wang[a,b,c], Bin Liu[a,b,c], Xiaoyan Shao[a,b,c], Yi He[a,b,c], Na Liu[a,b,c], Jiaquan Lin[a,b,c], Jianghui Qin[a,b,c], Qing Jiang[a,b,c,d,*], Baosheng Guo[a,b,c,*]

[a]*Division of Sports Medicine and Adult Reconstructive Surgery, Department of Orthopedic Surgery, Nanjing Drum Tower Hospital, Affiliated Hospital of Medical School, Nanjing University, Nanjing 210008, China*
[b]*State Key Laboratory of Pharmaceutical Biotechnology, Nanjing University, Nanjing 210093, China*
[c]*Jiangsu Key Laboratory of Molecular Medicine, Medical School, Nanjing University, Nanjing 210093, China*
[d]*Branch of National Clinical Research Center for Orthopedics, Sports Medicine and Rehabilitation, Nanjing 210000, China*

Received 24 January 2025; received in revised form 10 March 2025; accepted 2 April 2025

KEY WORDS

Osteoarthritis (OA);
Senescent FLS;
Cartilage degradation;
Mitochondrial dysfunction;
Acetylation;
CRTAC1;
SIRT3;
FOXO3a

Abstract Osteoarthritis (OA), the most prevalent joint disease of late life, is closely linked to cellular senescence. Previously, we found that the senescence of fibroblast-like synoviocytes (FLS) played an essential role in the degradation of cartilage. In this work, single-cell sequencing data further demonstrated that cartilage acidic protein 1 (CRTAC1) is a critical secreted factor of senescent FLS, which suppresses mitophagy and induces mitochondrial dysfunction by regulating SIRT3 expression. *In vivo*, deletion of SIRT3 in chondrocytes accelerated cartilage degradation and aggravated the progression of OA. Oppositely, intra-articular injection of adeno-associated virus expressing SIRT3 effectively alleviated OA progression in mice. Mechanistically, we demonstrated that elevated CRTAC1 could bind with NRF2 in chondrocytes, which subsequently suppresses the transcription of SIRT3 *in vitro*. In addition, SIRT3 reduction could promote the acetylation of FOXO3a and result in mitochondrial dysfunction, which

*Corresponding authors.
E-mail addresses: qingj@nju.edu.cn (Qing Jiang), borisguo@nju.edu.cn (Baosheng Guo).
†These authors made equal contributions to this work.
Peer review under the responsibility of Chinese Pharmaceutical Association and Institute of Materia Medica, Chinese Academy of Medical Sciences.

https://doi.org/10.1016/j.apsb.2025.08.014

finally contributes to the degradation of chondrocytes. To conclude, this work revealed the critical role and underlying mechanism of senescent FLSs-derived CRTAC1 in OA progression, which provided a potential strategy for the OA therapy.

1. Introduction

Osteoarthritis (OA), the most prevalent age-related joint disease, is primarily characterized by disrupted articular cartilage homeostasis and subsequent degradation of the cartilage matrix[1]. As a prototypical degenerative disease, cellular senescence, the hallmark of aging, has been proposed as an essential driver in the pathogenesis of osteoarthritis[2]. Cellular senescence is a state of irreversible cell cycle arrest, characterized by resistance to apoptosis and persistent secretion of senescence-associated secretory phenotype (SASP) factors. In addition to chondrocytes, fibroblast-like synoviocytes (FLS), synovial macrophages, and adipocytes also contribute to SASP production[3]. In addition, it has been determined that senescent FLS secrete various SASPs, which ultimately lead to chondrocyte degeneration and OA progression both *in vivo* and *in vitro*[4]. As a physiologically non-self-renewing avascular tissue, the dysfunction of resident chondrocytes directly modulates the cartilage homeostasis[5]. Therefore, uncovering the underlying molecular mechanisms of senescent FLS-induced chondrocyte dysfunction in OA progression may offer innovative therapeutic strategies for mitigating or impeding the development of OA.

The cartilage is immersed in synovial fluid, which contains a variety of proteins that are responsible for maintaining normal joint function. In OA joints, alterations in the synovial fluid composition may facilitate chondrocyte degeneration by modulating its physicochemical properties[6]. In OA synovial fluid, there was a significant increase in the levels of cartilage acidic protein 1 (CRTAC1) compared to healthy synovial fluid[7], which was similarly upregulated in OA synovium[7,8]. CRTAC1 is initially identified as a gene induced during chondrogenesis, which is highly conserved in mouse and human[9,10]. In addition, CRTAC1 was recognized as a promising biomarker for OA, exhibiting a strong correlation with OA severity and serving as an accurate predictor of joint replacement progression[11,12]. It has been reported that CRTAC1 may function as a cytokine, promoting the catabolic activity and inhibiting the anabolic activity of chondrocytes in the development of OA[13]. However, the mechanisms by which CRTAC1 regulates OA progression remain unclear. In our work, we found CRTAC1 was profoundly increased in senescent FLS, and its expression positively correlates with cellular senescence. Exogenous treatment of CRTAC1 resulted in mitochondrial damage and impaired mitophagy. Emerging evidence has indicated that the imbalance of mitochondrial homeostasis results in oxidative stress and reactive oxygen species (ROS) overproduction, which contribute to the occurrence and progression of OA[14,15]. However, the role of CRTAC1 in mechanisms that regulate chondrocyte redox balance has yet to be fully elucidated.

OA cartilage is more susceptible to ROS damage due to a decrease in expression of mitochondrial antioxidant enzymes. Sirtuin 3 (SIRT3) is a deacetylase that plays an essential role in promoting mitochondrial dynamics and anti-oxidation to alleviate mitochondrial dysfunction[16]. Studies have shown that SIRT3 expression is decreased in the cartilage of mice with aging, and SIRT3 knockout accelerates the progression of OA. Oppositely, restoration of SIRT3 during aging could protect cartilage from DMM-induced degradation[17]. However, the role of SIRT3 in CRTAC1-mediated chondrocyte degeneration was not studied, and the underlying mechanism needs further investigation. In this study, we explored the essential role and underlying molecular mechanism of CRTAC1 in chondrocyte degeneration and OA progression. We performed single-cell RNA-sequencing (scRNA-seq) analysis in the normal and OA synovium, which indicated a positive correlation between CRTAC1 and senescent FLS. We identified that CRTAC1 suppressed mitophagy and promoted the mitochondrial damage of chondrocytes *via* impairing the transcription activity of FOXO3a, which subsequently modulated the expression of antioxidant and mitophagy-related genes. Further mechanism studies revealed that CRTAC1 directly binds to the transcription factor NRF2, and then suppresses NRF2-mediated SIRT3 transcription, which subsequently results in enhanced acetylation of FOXO3a. The elucidation of such mechanisms will potentially offer broader insights into the pathophysiology of OA and facilitate the development of new strategies for OA therapy.

2. Materials and methods

2.1. Reagents and antibodies

All chemical small molecules were procured from MedChemExpress (Shanghai, China), including nicotinamide (NAM, catalog no. HY-B0150) and trichostatin A (TSA, catalog no. HY-15144). Detailed information regarding the antibodies utilized in this study can be found in Supporting Information Table S1.

2.2. Animal experiments

COL2A1-CreER mice were purchased from Gempharmatech (Nanjing, China). The Cre recombination efficiency could be induced with tamoxifen administration. *SIRT3*$^{flox/flox}$ mice were also obtained from Gempharmatech and were further bred with *COL2A1-CreER* mice to generate the inducible conditional Sirt3 knockout mice (*COL2A1-CreER; SIRT3*$^{flox/flox}$ mice). For conditional knockout of the Sirt3 gene in chondrocytes (Supporting Information Fig. S6D), *COL2A1-CreER*; *SIRT3*$^{flox/flox}$ mice were administered with tamoxifen (Sigma−Aldrich, MO, USA) 100 mg/kg per day intraperitoneally at the age of 3 months, 5 days before DMM surgery. Mice treated with corn oil were used as controls in this study. All C57BL/6 genetic background mice used were housed in a specific pathogen-free (SPF) environment. And the procedures were strictly performed according to the protocols approved by the Institutional Animal Care and Use Committee of Nanjing University (IACUC-D2202120).

For OA induction, the right knees of male mice aged 3 months underwent either destabilization of the medial meniscus (DMM) surgery or sham surgery, following a previously described protocol[4]. Briefly, mice were anesthetized and the joint capsule was opened shortly under type microscope. The medial meniscotibial ligament was intentionally severed without causing harm to adjacent tissues. In the sham group, the joint capsule was opened without additional damage. For local delivery, mice were intra-articularly injected with 10 μL of recombinant adeno-associated virus (AAV) containing specified siRNA or genes (1×10^{11} GC) 14 days post-DMM surgery. The joint samples were collected at 8 weeks after DMM. The number of mice in each group was calculated according to the formula reported by Charan and Kantharia[18].

2.3. Histology and immunohistochemistry

Mouse knee joints were fixed overnight with 4% paraformaldehyde and then decalcified with ethylene diamine tetraacetic acid (EDTA) before paraffin embedding. The paraffin-embedded samples were sectioned into 5 μm slices for Fast Green and Safranin O staining. Cartilage destruction was assessed by blinded observers using the Osteoarthritis Research Society International (OARSI) grading system (0-6). The highest OARSI score for every section was recorded, and the means of all scores were calculated[19]. For immunohistochemistry, sections underwent deparaffinization in xylene and rehydration through an ethanol gradient to water. Antigen retrieval was performed after washing, followed by incubation with 3% hydrogen peroxide (H_2O_2) to quench endogenous peroxidase activity. Sections were then blocked with goat serum to reduce non-specific binding. Next, the sections were incubated overnight at 4 °C with the specified primary antibodies. Following this, they were washed and incubated with the appropriate secondary antibody for 1 h at room temperature. Antigen-positive cells were detected using a DAB Substrate kit (ZSGB-BIO, Beijing, China). The proportions of positive cells in human synovium were calculated by two observers under a blind condition.

2.4. Immunofluorescent staining

For immunofluorescent staining, fixed cells or deparaffinized tissues were first permeabilized with 0.3% Triton X-100 at room temperature for 5 min. Following this, samples were blocked with bovine serum albumin (BSA; Sigma) at room temperature for 1 h. Then, the samples were incubated with primary antibodies overnight at 4 °C. After washing with PBS five times, the samples were incubated with fluorescently labeled secondary antibodies specific to the host species of the primary antibody for 1 h at room temperature. The Nuclei were counterstained with DAPI (Beyotime Biotechnology, Shanghai, China). Images were captured using a confocal laser scanning microscope (Olympus).

2.5. Isolation of FLS and cell culture

Synovium specimens for this study were collected from patients diagnosed with OA and from control subjects without synovitis or cartilage injury. OA synovium samples were obtained from 10 patients (aged 50−65 years) undergoing total knee replacement surgery in Nanjing Drum Tower Hospital (Nanjing, China). Normal synovium samples were sourced from 10 patients (aged 50−65 years) undergoing arthroscopic meniscus repair surgery, confirmed to have no synovitis or cartilage injury *via* arthroscopic examination. This study was approved by the Ethical Committee of the Nanjing Drum Tower Hospital (2020-156-01). The synovial tissues were enzymatically digested with collagenase A (2 mg/mL) and DNase I (0.1 mg/mL; Roche) to isolate the fibroblast-like synoviocytes (FLS). The FLSs were further cultured in Dulbecco's modified Eagle's medium (DMEM) supplemented with 10% fetal bovine serum (FBS). The next day, the non-adherent cells were removed, and the cells were passaged using Trypsin-EDTA (Gibco) when they reached approximately 90% confluence and subcultured in fresh medium.

The human chondrocyte cell line C28/I2 was established by Professor Mary B. Goldring's laboratory at the Hospital for Special Surgery/Weill Medical College of Cornell University. These cells, isolated from the costal cartilage of a 15-year-old female, were immortalized using SV-40 large T-antigen[20]. C28/I2 cells were maintained in DMEM/F12 medium supplemented with 10% FBS. Similar to the FLS culture protocol, cells were passaged using Trypsin-EDTA (Gibco) upon reaching about 90% confluence and transferred to fresh medium.

2.6. RNA interference

The lentivirus-based vectors were used for regulating the expression of CRTAC1, FOXO3a, or SIRT3 (OBIO, Shanghai, China). The siRNA sequences used against CRTAC1 or SIRT3 were listed as follows: mouse CRTAC1, 5′- GCACCTAC GGATCATTGAT-3′; human CRTAC1, 5′- CTCTATCTACATTGC CAATTA-3′; human SIRT3, 5′- CCCAACGTCACTCA CTACTTT-3′. Lentiviruses were produced in accordance with the protocol provided by the manufacturer. The viruses were employed for cell infection in the presence of protamine sulfate at a concentration of 8 μg/mL.

2.7. Western blot analysis

For the detection of protein levels, cells or tissues were lysed on ice for 30 min using RIPA buffer supplemented with protease and phosphatase inhibitor cocktails (KeyGen Biotech, Nanjing, China). Protein concentrations were detected using the BCA protein assay kit (Beyotime Biotechnology, Shanghai, China). The total proteins were separated by SDS-PAGE before transferring onto polyvinylidene difluoride (PVDF) membranes (Millipore). Then, the membranes were washed and blocked with 5% non-fat milk at room temperature for 1 h. Following blocking, the membranes were incubated with the appropriate primary antibodies overnight at 4 °C. After five washes with PBST, the membranes were incubated with horseradish peroxidase (HRP)-conjugated secondary antibodies. Protein bands were further visualized by an automatic chemiluminescence imaging system (Tanon, Shanghai, China) after incubation with an enhanced chemiluminescence solution (Millipore). The protein levels were determined by quantification of the intensity of each band using ImageJ software and normalized to ACTB.

2.8. Quantitative real-time PCR

RNAs were extracted from cells or tissues using TRIzol reagent (KeyGen Biotech, Nanjing, China) according to the manufacturer's instructions. Complementary DNAs (cDNAs) were acquired from the isolated RNA using the HiScript Q RT SuperMix (Vazyme, Nanjing, China). The ChamQ SYBR qPCR Master Mix

(Vazyme) on an ABI StepOne Plus™ Real-Time PCR System (Applied Biosystems) was used for detecting the mRNA levels, which were quantified using the $2^{-\Delta\Delta Ct}$ method. Primer sequences are provided in Supporting Information Tables S2 and S3.

2.9. SA-β-Gal staining

For cellular senescence detection, the Cell Senescence β-Galactosidase Staining Kit (Beyotime Biotechnology) was used to stain senescent FLS. Briefly, tissues were washed and fixed with 2% paraformaldehyde and 0.2% glutaraldehyde for 5 min. Then, the samples were washed and further incubated with the SA-β-Gal staining solution at 37 °C for 16 h. Senescent cells were imaged using an Eclipse Ni-U microscope (Nikon). Total cells and SA-β-Gal−Gal-positive cells were calculated in six random fields per culture dish by two observers under blind conditions *via* ImageJ.

2.10. ROS and mitochondrial membrane potential assay

The expression of ROS was detected by ROS Assay Kit -Highly Sensitive DCFH-DA and MitoBright ROS Deep Red (Dojindo, Shanghai, China). Briefly, C28/I2 cells with the indicated treatment were incubated with Highly Sensitive DCFH-DA Dye (1 μmol/L) or MitoBright ROS Deep Red working solution (10 μmol/L) for 30 min at 37 °C. Cells were washed twice with PBS and analyzed by a laser confocal scanning microscope (Olympus).

The mitochondrial membrane potential was measured using the JC-1 MitoMP Detection Kit (Dojindo, Shanghai, China). Briefly, C28/I2 cells were washed with PBS and subsequently incubated with JC-1 in a 37 °C incubator for 30 min. Then, cells were washed with PBS twice and covered with imaging buffer solution. Subsequently, the cells were imaged with a laser confocal scanning microscope (Olympus).

2.11. Immunoprecipitation

For immunoprecipitation experiments, cells were lysed with a buffer containing a protease inhibitor cocktail. Lysates were rotated at 4 °C for 1 h with intermittent vortexing and were centrifuged at 5000×*g* for 5 min to remove the cellular debris. The supernatant was incubated with FOXO3a or NRF2 antibody-conjugated Pierce Protein A/G Magnetic Beads (Thermo Fisher Scientific). Following three washes with lysis/wash buffer, protein complexes were eluted by incubating with low pH elution buffer for 10 min. The beads were magnetically separated, and the supernatant containing the target antigen was collected for further immunoblotting analysis.

2.12. ELISA

Cells were rinsed with phosphate-buffered saline (PBS) and cultured in serum-free DMEM supplemented with antibiotics for 48 h. The resulting conditioned medium was filtered and stored at −80 °C. Cell counts were determined for each experiment. ELISAs were conducted using kits from Boster Biological Technology, and the data were normalized based on the number of cells present.

2.13. Statistical analysis

Results are expressed as the mean ± standard error of the mean (SEM). Statistical analyses were performed using Student's *t*-test for comparisons between two groups and one-way ANOVA followed by *post hoc* tests for multiple group comparisons, as detailed in the figure legends. *P* values were considered statistically significant at $^{*}P < 0.05$ and $^{**}P < 0.01$.

3. Results

3.1. CRTAC1 is elevated in the FLS of OA patients

Considering the critical role of synovium in the development of OA, we generated single-cell suspensions from the synovium of OA patients and non-OA controls (Normal), and then performed scRNA-seq using the 10 × Genomics Chromium platform. We removed low-quality cells according to the inclusion criteria for cells based on observations from the entire dataset. A total of 32,161 cells underwent dimensionality reduction and unsupervised clustering (9178 cells for control, 22,983 cells for OA) using Seurat[21]. As illustrated in Supporting Information Fig. S1A and S1B, we annotated and classified 18 clusters into five distinct cell types within the synovium based on canonical lineage-defining markers (Supporting Information Table S4), including fibroblasts, macrophages, smooth muscle cells, endothelial cells, and NK cells (Fig. 1A). As previously reported, OA FLS have been shown to induce the degradation of cartilage both *in vivo* and *in vitro*[4]. To better define the underlying mechanism of OA-FLS-mediated cartilage degradation in OA progression, differentially expressed genes within the fibroblast cluster were identified using the Wilcoxon rank-sum test with a significance cutoff of $P < 0.01$ and evaluated by Ingenuity Pathway Analysis (IPA). Our results showed that CRTAC1 was significantly elevated in OA synovium (Supporting Information Fig. S2A and S2B), which was highly expressed in OA FLS as compared with the fibroblasts originating from normal synovium (Fig. 1B−D, Fig. S1C and S1D). Sub-clustering of fibroblasts resulted in 13 distinct clusters (Fig. S1E and S1F), which also showed that CRTAC1 was profoundly elevated in OA fibroblasts (Fig. 1E). To verify the results of scRNA-seq, we also observed an elevated expression of CRTAC1 and senescence markers both in OA synovium and OA FLS (Fig. 1F−J). The immunofluorescence-based analysis of co-localization also demonstrated that CRTAC1 was dramatically increased in $p16^{INK4a}$-positive cells (Fig. 1K). These results indicated that CRTAC1 is highly expressed in senescent FLS.

3.2. Clearance of senescent FLS suppresses CRTAC1 expression in vitro and in vivo

To further confirm the relationship between FLS senescence and CRTAC1 expression in OA progression, OA-FLS was treated with ABT-263, which can selectively clear senescent cells[22]. Treatment with ABT-263 significantly reduced the levels of $p16^{INK4a}$ and p21, along with decreased expression of CRTAC1, which indicated that clearance of senescent FLS could suppress the production of CRTAC1 (Fig. 2A and B, Fig. S2C). In addition, inducing the senescence of FLS *via* bleomycin administration could also promote the expression and secretion of CRTAC1, which could be compromised with the treatment of ABT-263 (Fig. 2C and D, Fig. S2D). *In vivo*, we established a DMM-induced OA model in INK-ATTAC transgenic mice that expresses FKBP-Casp8 and GFP under the control of a minimal $p16^{INK4a}$ promoter fragment transcriptionally active in senescent cells and monitored cell survival after activating the FKBP-Casp8

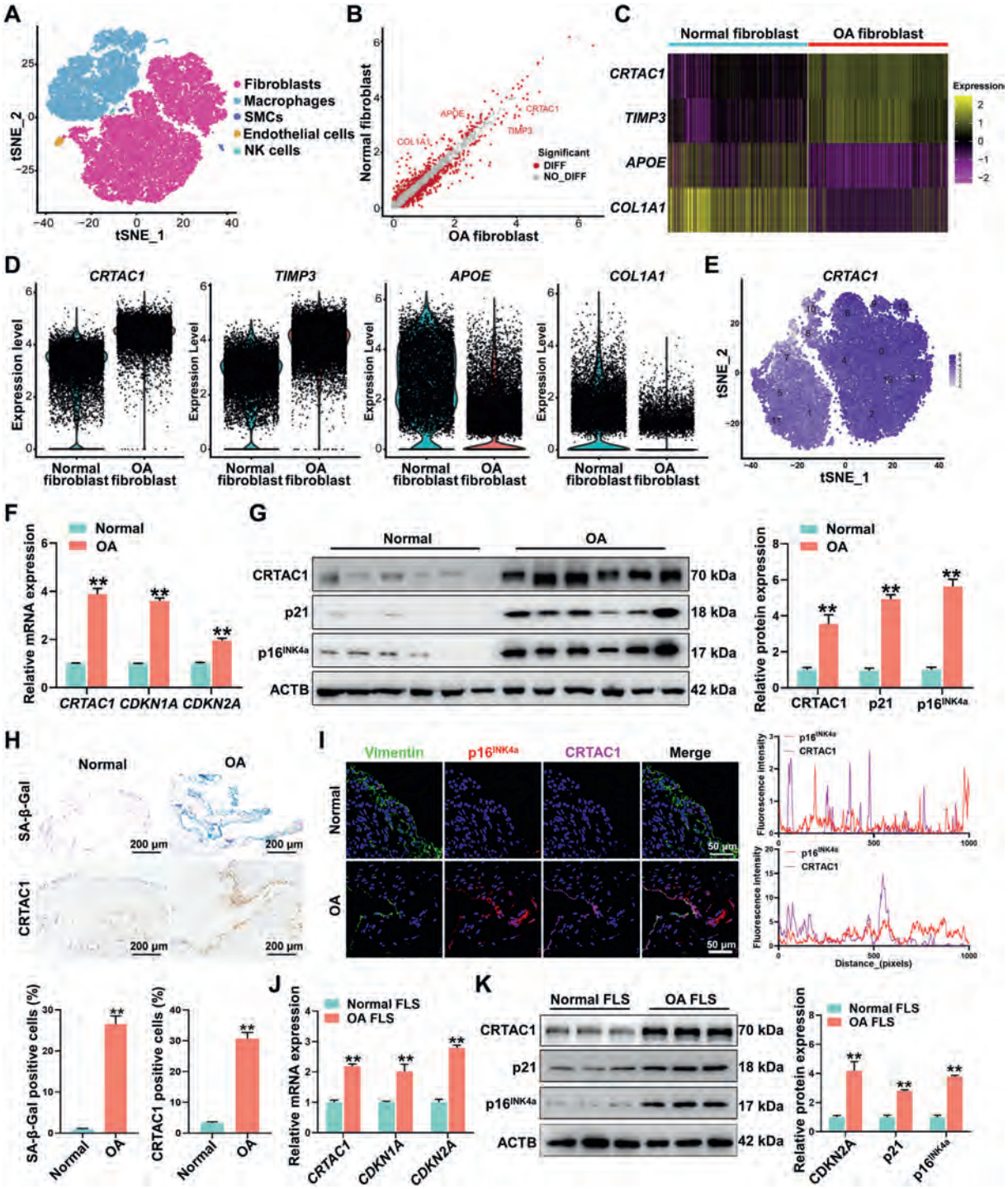

Figure 1 CRTAC1 is elevated in the FLS of OA patients. (A) tSNE plots of all cells analyzed from human normal synovium (9178 cells) and OA synovium (22,983 cells), colored by density clustering and annotated by cell-type identity. (B) Scatter plots showing the differentially expressed genes from OA synovium versus normal synovium. (C) Heatmap revealing the scaled expression of *CRTAC1*, *TIMP3*, *APOE*, and *COL1A1* in the fibroblasts cluster defined in A. (D) Violin plots showing the expression levels of *CRTAC1*, *TIMP3*, *APOE*, and *COL1A1* for fibroblasts. (E) Feature plots demonstrating expression of CRTAC1 in fibroblasts from normal synovium and OA synovium. (F) qPCR analysis of the expression of *CRTAC1*, *CDKN1A*, and *CDKN2A* in the synovium from OA patients and patients without OA (Normal). $n = 10$, $^{**}P < 0.01$. (G) Western blot analysis of the protein levels of CRTAC1, p21, and $p16^{INK4a}$ in the normal synovium and OA synovium. $n = 6$, $^{**}P < 0.01$. (H) Representative images and analysis of SA-β-Gal staining (up panel) and immunostaining (lower panel) for CRTAC1 in the normal synovium and OA synovium. $n = 6$. $^{**}P < 0.01$. (I) Representative images and analysis of coimmunostaining of vimentin, $p16^{INK4a}$, and CRTAC1 in the normal synovium and OA synovium. (J) qPCR analysis of the expression of *CRTAC1*, *CDKN1A*, and *CDKN2A* in normal FLS and OA FLS. $n = 3$, $^{**}P < 0.01$. (K) Western blot analysis of the protein levels of CRTAC1, p21, and $p16^{INK4a}$ in normal FLS and OA FLS. $n = 3$, $^{**}P < 0.01$. All data are presented as the mean ± SEM. A paired *t*-test was used for statistical analysis.

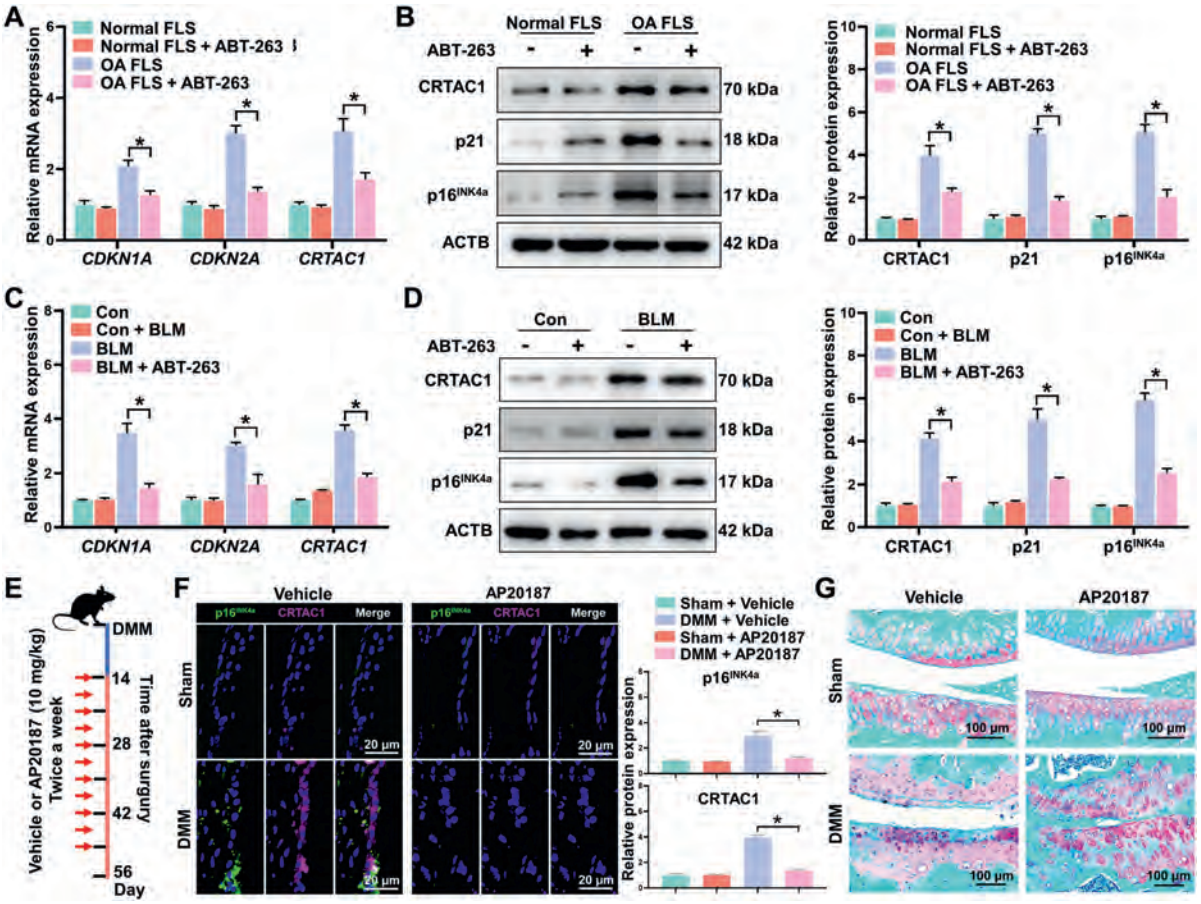

Figure 2 Clearance of senescent FLS suppresses CRTAC1 expression *in vitro* and *in vivo*. (A) qPCR analysis of the expression of *CRTAC1*, *CDKN1A*, and *CDKN2A* in normal FLS and OA FLS treated with or without ABT-263 (2 μmol/L). $n = 3$, $^*P < 0.05$. (B) Western blot analysis of the expression of CRTAC1, p21, and $p16^{INK4a}$ in normal FLS and OA FLS treated with or without ABT-263. $n = 3$, $^*P < 0.05$. (C) qPCR analysis of the expression of *CRTAC1*, *CDKN1A*, and *CDKN2A* in FLS pretreated with bleomycin (BLM), accompanied with or without ABT-263 (2 μmol/L) treatment. $n = 3$, $^*P < 0.05$. (D) Western blot analysis of the expression of CRTAC1, p21, and $p16^{INK4a}$ in FLS pretreated with BLM, accompanied with or without ABT-263 treatment. $n = 3$, $^*P < 0.05$. (E) Schematic of the time course for the experiments in F and G. (F) Representative images and analysis of coimmunostaining of $p16^{INK4a}$ and CRTAC1 in the knee joint from post-traumatic *INK-ATTAC* transgenic mice intraperitoneally injected with or without AP20187 (10 mg/kg). $n = 6$, $^*P < 0.05$. (G) The representative safranin O staining images of the knee joints from post-traumatic *INK-ATTAC* transgenic mice intraperitoneally injected with or without AP20187. $n = 6$. All data are presented as the mean ± SEM. One-way ANOVA with Tukey's *post hoc* test (A)−(F) was used for statistical analysis.

fusion protein by AP20187 treatment (Fig. 2E)[23]. AP20187 treatment markedly reduced $p16^{INK4a}$ and CRTAC1 expression, which were profoundly elevated in the synovium of OA mice (Fig. 2F). In addition, clearance of senescent cells by AP20187 also inhibited articular cartilage erosion as confirmed by safranin O staining for proteoglycans (Fig. 2G). These results suggested that elevated CRTAC1 expression is tightly correlated with FLS senescence, which may play an essential role in senescent cell-mediated cartilage degradation in OA progression.

3.3. OA FLS-mediated degradation of chondrocytes depends on the secretion of CRTAC1

To confirm whether CRTAC1 participated in OA pathogenesis, synovial fluid ($n = 5$ healthy, $n = 5$ OA) was analyzed using high-resolution liquid chromatography mass spectrometry (LC−MS). Differential abundance analyses were conducted to detect dysregulated proteins in OA synovial fluid. In total, 1004 proteins were detected and relatively quantified in synovial fluid samples from 5 OA and 5 normal subjects. Among them, 5 proteins were significantly upregulated and 15 proteins were significantly downregulated in OA synovial fluid (Fig. 3A, Supporting Information Fig. S3A and S3B). Interestingly, we found that CRTAC1 was significantly elevated in OA synovial fluid (Fig. 3B). *In vitro*, we detected increased expression of MMP13 and decreased levels of Collagen II in C28/I2 cells after CRTAC1 treatment (Fig. 3C−E). To further verify whether OA FLS-mediated chondrocyte dysfunction was due to elevated CRTAC1 expression, FLS were transfected with *CRTAC1 siRNA* before being co-cultured with C28/I2 cells. Knockdown of CRTAC1 effectively attenuated the expression and secretion of CRTAC1 in OA-FLS (Fig. 3F, Fig. S3C). The expression of MMP13 was profoundly decreased, and Collagen II expression was dramatically elevated in C28/I2 cells that were co-cultured with *CRTAC1 siRNA*-transfected OA FLS as compared with cells co-cultured with OA-FLS (Fig. 3G). Our results demonstrated that suppression of CRTAC1 effectively abrogated OA FLS-induced degradation of chondrocytes. *In vivo*, we observed decreased safranin O

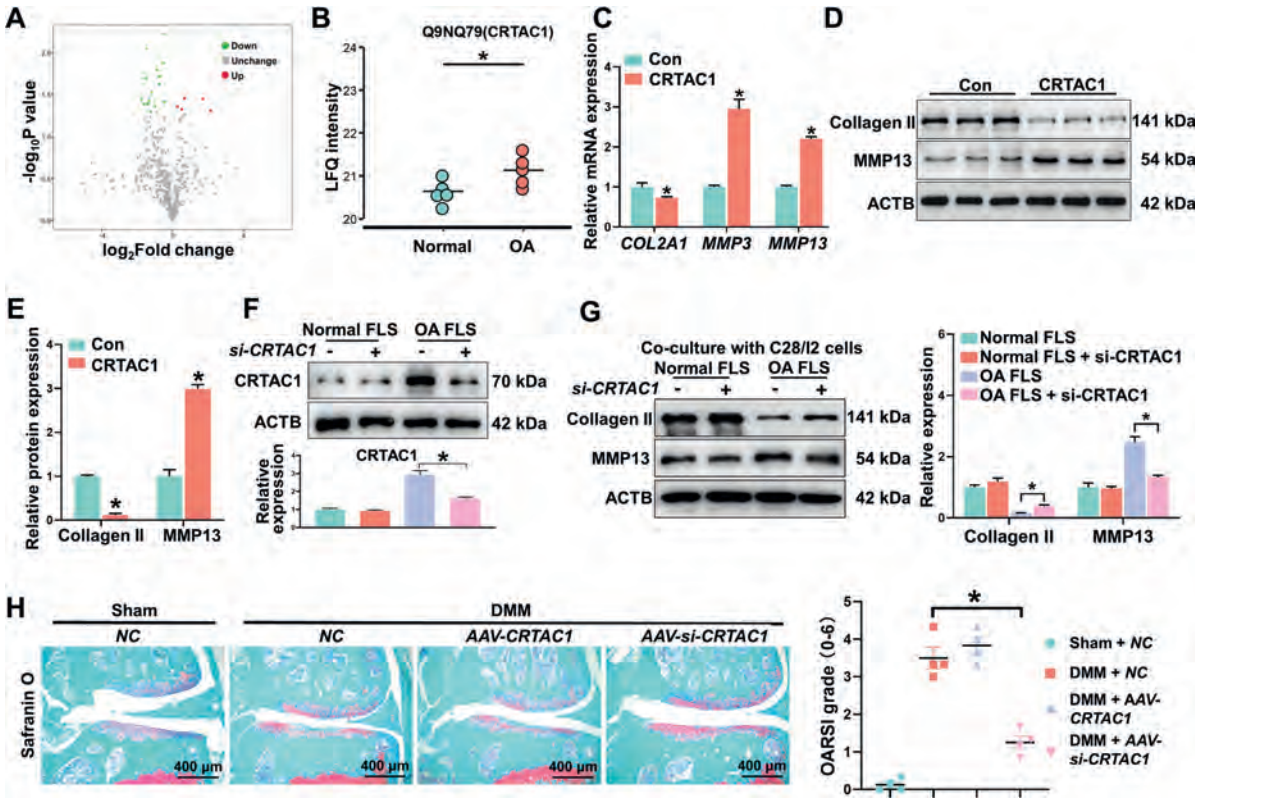

Figure 3 CRTAC1 induces the degradation of chondrocytes *in vivo* and *in vitro.* (A) Volcano plots showing differentially expressed proteins detected by LC−MS in OA synovium fluid versus normal synovium fluid. (B) The protein levels of CRTAC1 based on the LFQ intensity in normal and OA synovium fluid. $n = 5$, $^*P < 0.05$. (C) qPCR analysis of the expression of *COL2A1*, *MMP3* and *MMP13* in C28/I2 cells treated with or without recombinant CRTAC1 (100 ng/mL). $n = 3$, $^*P < 0.05$. (D, E) Western blot analysis of the expression of Collagen II and MMP13 in C28/I2 cells treated with or without recombinant CRTAC1 (100 ng/mL). $n = 3$, $^*P < 0.05$. (F) Western blot analysis of CRTAC1 levels in normal FLS and OA FLS transfected with or without *CRTAC1 siRNA* (*si-CRTAC1*). $n = 3$, $^*P < 0.05$. (G) Western blot analysis of the expression of Collagen II and MMP13 in C28/I2 cells that were co-cultured with FLS treated as in (F). $n = 3$, $^*P < 0.05$. (H) The representative safranin O staining images and analytical results with the Osteoarthritis Research Society International (OARSI) scoring system of the knee joints from DMM mice intra-articular injected with *AAV-NC*, *AAV-CRTAC1*, or *AAV-si-CRTAC1*. $n = 6$, $^*P < 0.05$. All data are presented as the mean ± SEM. Paired *t*-test (B) and (C) and one-way ANOVA with Tukey's *post hoc* test (D)−(H) were used for statistical analysis.

staining and aggravated cartilage degradation in mice injected with *AAV-CRTAC1* (Fig. 3H, Fig. S3D). Oppositely, the progressive cartilage degradation in DMM mice was significantly reversed after intra-articular administration of *AAV-si-CRTAC1* (Fig. 3H, Fig. S3E). These results indicated that senescent FLS-mediated degradation of cartilage was dependent on the secretion of CRTAC1 in OA progression.

3.4. CRTAC1 induces mitochondrial dysfunction of chondrocytes in a FOXO3a-dependent manner

To further uncover CRTAC1-mediated pathophysiology in chondrocytes, C28/I2 cells were treated with CRTAC1, and morphological alterations in mitochondria and autophagosomes were determined by TEM. We observed a decreased number of autophagosomes in CRTAC1-treated C28/I2 cells (Supporting Information Fig. S4). The mitochondria's shape was altered from oblong to swollen, and the regular pattern of the cristae was impaired after CRTAC1 treatment (Fig. 4A). Moreover, the mitochondrial membrane potential was measured through the JC-1 assay, the results of which showed that CRTAC1 could accelerate mitochondrial damage *in vitro* (Fig. 4B and D). Mitochondria are important cellular organelles which was the main source of cellular ROS. Accumulation of excessive ROS in mitochondria would result in cellular oxidative stress, which may damage mitochondria[24]. Thus, the total intracellular ROS levels and mitochondrial ROS were measured by DCF-DA assay and Mito-SOX assay, respectively. ROS staining showed that the DCF-DA (green) and Mito-SOX (pink) fluorescent levels were extensively augmented in C28/I2 cells following the administration of CRTAC1 (Fig. 4C and E), which indicated that CRTAC1 could enhance the production of mitochondrial ROS. Recently, FOXO3a was reported to be tightly associated with mitochondrial-derived ROS and mitophagy *via* modulating the transcription of antioxidant enzymes and mitophagy-related genes[25-28], which was robustly impaired in the cartilage of OA mice (Fig. 4F). *In vitro*, we observed a significant decrease in the protein levels of FOXO3a in CRTAC1-treated C28/I2 cells (Fig. 4H). Additionally, there was a notable reduction in SOD2, Parkin, and LC3 expression (Fig. 4G and H). To confirm the role of FOXO3a in CRTAC1-mediated chondrocyte mitochondrial dysfunction, C28/I2 cells were transfected with *LV-FOXO3a* in the presence or absence of CRTAC1 treatment. The findings demonstrated that the upregulation of FOXO3a effectively enhanced the expression of SOD2,

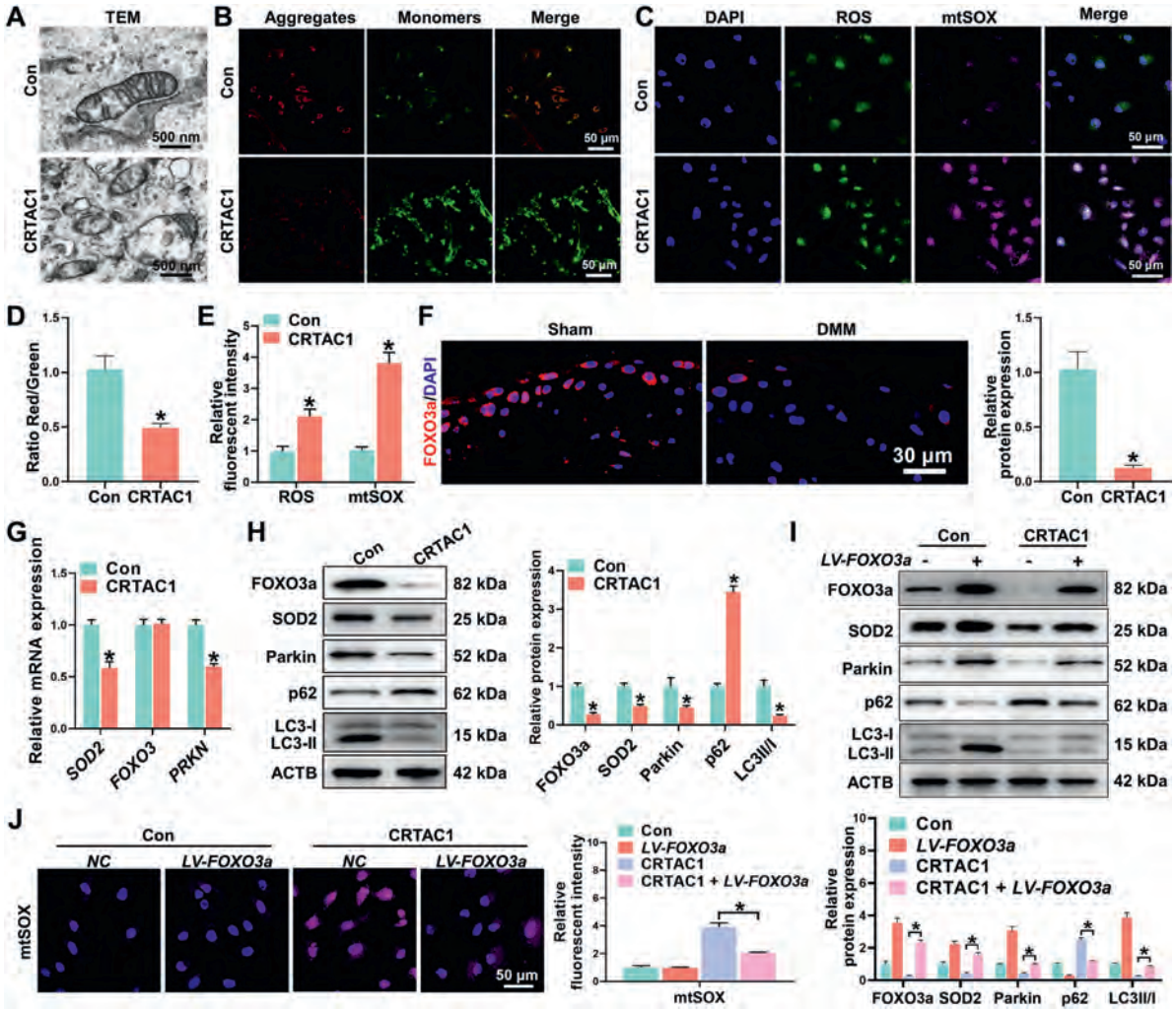

Figure 4 CRTAC1 induces mitochondrial dysfunction of chondrocytes in a FOXO3A-dependent manner. (A) Representative transmission electron microscope (TEM) images showing mitochondrial morphology in C28/I2 cells treated with or without recombinant CRTAC1. (B, D) The detection and analysis of mitochondrial potential changes by JC-1 staining in C28/I2 cells treated with or without recombinant CRTAC1. $n = 3$, $^*P < 0.05$. (C, E) The detection and analysis of ROS and mtSOX expression in C28/I2 cells treated with or without recombinant CRTAC1. $n = 3$, $^*P < 0.05$. (F) Immunofluorescence staining and analysis of FOXO3a in the cartilage from mice suffered with DMM surgery. $n = 6$, $^*P < 0.05$. (G) qPCR analysis of the expression of *SOD2*, *FOXO3a* and *PRKN* in C28/I2 cells treated with or without recombinant CRTAC1. $n = 3$, $^*P < 0.05$. (H) Western blot analysis of the expression of FOXO3a, SOD2, Parkin, p62, and LC3 in C28/I2 cells treated with or without recombinant CRTAC1. $n = 3$, $^*P < 0.05$. (I) Western blot analysis of the expression of FOXO3a, SOD2, Parkin, p62, and LC3 in CRTAC1-treated C28/I2 cells transfected with or without lentivirus FOXO3a (*LV-FOXO3a*). $n = 3$, $^*P < 0.05$. (J) The detection and analysis of mtSOX expression in CRTAC1-treated C28/I2 cells transfected with or without *LV-FOXO3a*. $n = 3$, $^*P < 0.05$. All data are presented as the mean ± SEM. Paired *t*-test (D−H) and one-way ANOVA with Tukey's *post hoc* test (I, J) were used for statistical analysis.

Parkin, and LC3 (Fig. 4I), while simultaneously reducing mtSOX expression and increasing the clearance of damaged mitochondria (Fig. 4J, Fig. S4). These results suggested that overexpression of FOXO3a can enhance mitophagy and reverse the mitochondrial dysfunction caused by CRTAC1.

3.5. CRTAC1 induces the acetylation of FoxO3a in SIRT3-dependent manner

Intriguingly, we observed that CRTAC1 remarkably decreased the protein levels of FOXO3a without altering the mRNA expression (Fig. 4G). In addition, the nuclear expression of FOXO3a was dramatically decreased in CRTAC1-treated C28/I2 cells (Fig. 5A and B), which indicated the participation of post-translational modifications (PTMs). PTMs are fundamental processes that regulate protein function, potentially altering their subcellular localization, molecular stability, and DNA-binding affinity[25]. FOXO3a activity, in particular, is modulated by several types of PTMs, including phosphorylation, acetylation, ubiquitination, and methylation[29]. It was demonstrated that lysine 242 and 245 have been identified as two major acetylation modification residues in FOXO3a protein, which are near the nuclear localization signal (NLS) of FOXO family proteins and involved in FOXO3a-mediated transcriptional activation[30,31]. *In vitro*, treatment with CRTAC1 significantly induced FOXO3a acetylation (Fig. 5C and D). Interestingly, we found that the acetylation levels of FOXO3a were dramatically increased in C28/I2 cells after the SIRT inhibitor NAM treatment, but not in cells treated with trichostatin A

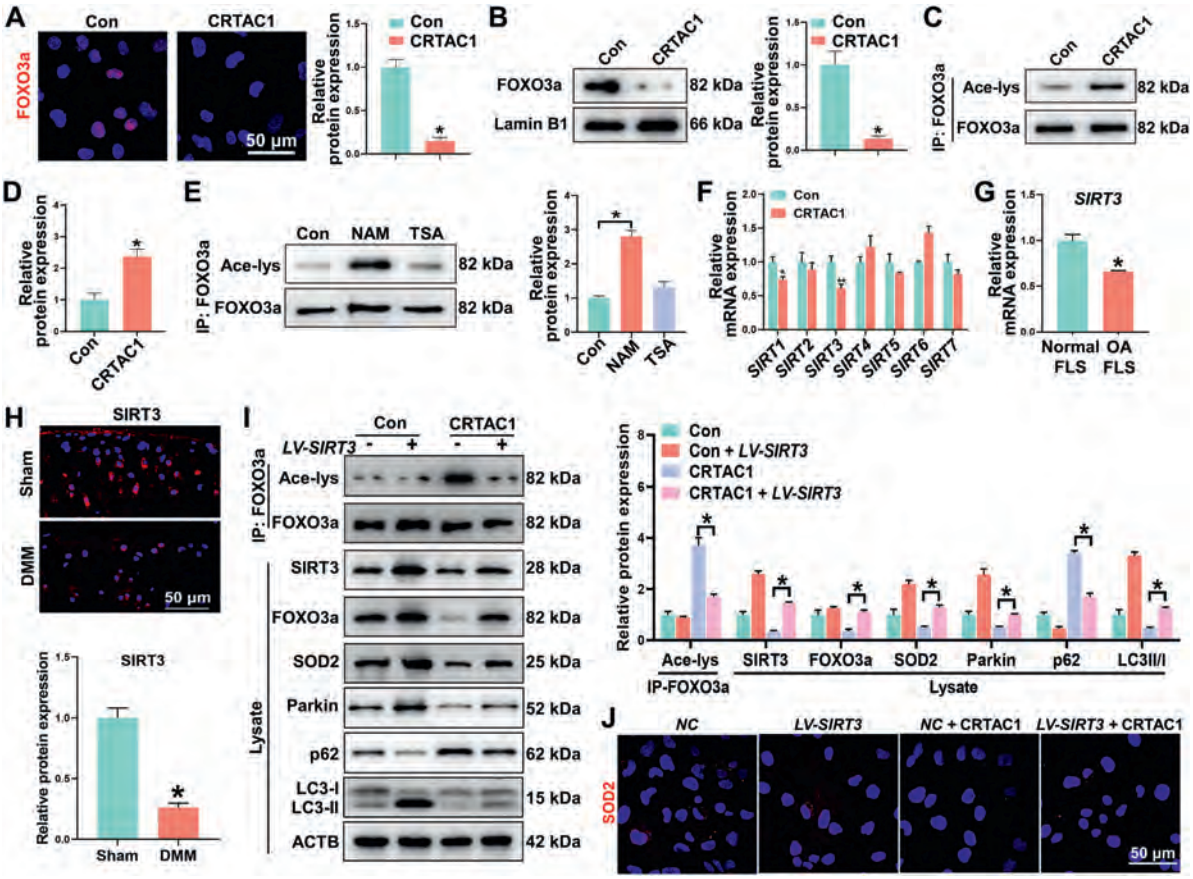

Figure 5 CRTAC1 induces the acetylation of FoxO3a in a SIRT3-dependent manner. (A) Immunofluorescence staining and analysis of FOXO3a in C28/I2 cells treated with or without recombinant CRTAC1. $n = 3$, $^*P < 0.05$. (B) Western blot analysis of the nuclear expression of FOXO3a in C28/I2 cells treated with or without recombinant CRTAC1. $n = 3$, $^*P < 0.05$. (C, D) Western blot analysis of the acetylation of FOXO3a in C28/I2 cells treated with or without recombinant CRTAC1. $n = 3$, $^*P < 0.05$. (E) Western blot analysis of the acetylation of FOXO3a in C28/I2 cells treated with nicotinamide (NAM) or trichostatin A (TSA). $n = 3$, $^*P < 0.05$. (F) qPCR analysis of the expression of *SIRT1-7* in C28/I2 cells treated with or without recombinant CRTAC1. $n = 3$, $^*P < 0.05$, $^{**}P < 0.01$. (G) qPCR analysis of the expression of SIRT3 in C28/I2 cells co-cultured with normal FLS or OA FLS. $n = 3$, $^*P < 0.05$. (H) Immunofluorescence staining and analysis of FOXO3a in the cartilage from mice suffered with DMM surgery. $n = 6$, $^*P < 0.05$. (I) Western blot analysis of the acetylation of FOXO3a, SIRT3, FOXO3a, SOD2, Parkin, p62, and LC3 expression in recombinant CRTAC1-treated C28/I2 cells transfected with or without *LV-SIRT3*. $n = 3$, $^*P < 0.05$. (J) Immunofluorescence staining of SOD2 in recombinant CRTAC1-treated C28/I2 cells transfected with or without *LV-SIRT3*. $n = 3$, $^*P < 0.05$. All data are presented as the mean ± SEM. Paired *t*-test (A−H) and one-way ANOVA with Tukey's *post hoc* test (I) were used for statistical analysis.

(TSA), an inhibitor of HDAC family deacetylases (Fig. 5E), which suggested the involvement of SIRT family deacetylases in FOXO3a acetylation. Thus, we further detected the expression of SIRT1-7 in CRTAC1-treated C28/I2 cells, in which SIRT3 was robustly decreased at the mRNA level (Fig. 5F). In addition, we observed an extensive reduction of SIRT3 expression in C28/I2 cells co-cultured with OA-FLS and in the cartilage of DMM-induced OA mice (Fig. 5G and H). It was reported that the deacetylase SIRT3 could promote both the activity and nuclear translocation of FOXO3a through its deacetylation ability[32,33]. To define whether SIRT3 is responsible for CRTAC1-induced FOXO3a acetylation, C28/I2 cells were overexpressed with SIRT3. We observed that upregulation of SIRT3 effectively decreased CRTAC1-mediated acetylation of FOXO3a (Fig. 5I), accompanied by elevated expression of SOD2, Parkin, and LC3 (Fig. 5I and J, Supporting Information Fig. S5). These results indicated that upregulating SIRT3 could restore CRTAC1-mediated mitophagy and mitochondrial dysfunction in chondrocytes.

3.6. SIRT3 knockdown in chondrocytes promotes FOXO3a acetylation and aggravates the progression of OA

To examine whether SIRT3 regulated the de-acetylation of FOXO3a, we suppressed the activity of SIRT3 in C28/I2 cells with 3-TYP treatment, and found that FOXO3a acetylation was robustly elevated, along with aggravated mitochondrial dysfunction (Fig. 6A and B, Supporting Information Fig. S6A). Endogenously knocking down SIRT3 expression could also induce the acetylation of FOXO3a *in vitro* (Fig. 6C), subsequently resulting in attenuated SOD2, Parkin, LC3, and Collagen II expression (Fig. 6E). MitoSOX staining also demonstrated increased ROS levels in chondrocytes transfected with *SIRT3 siRNA* (Fig. 6D). Subsequently, we established cartilage-specific $SIRT3^{-/-}$ mice *via* tamoxifen (TAM)-inducible Cre/loxP system to investigate the role of SIRT3 in OA progression. We mated $SIRT3^{flox/flox}$ mice with $COL2A1\text{-}Cre^{ERT2}$ mice and generated $COL2A1\text{-}Cre^{ERT2}/SIRT3^{flox/flox}$ ($SIRT3^{cKO}$) male littermates. Immunohistochemistry showed that SIRT3-positive cells were significantly reduced and

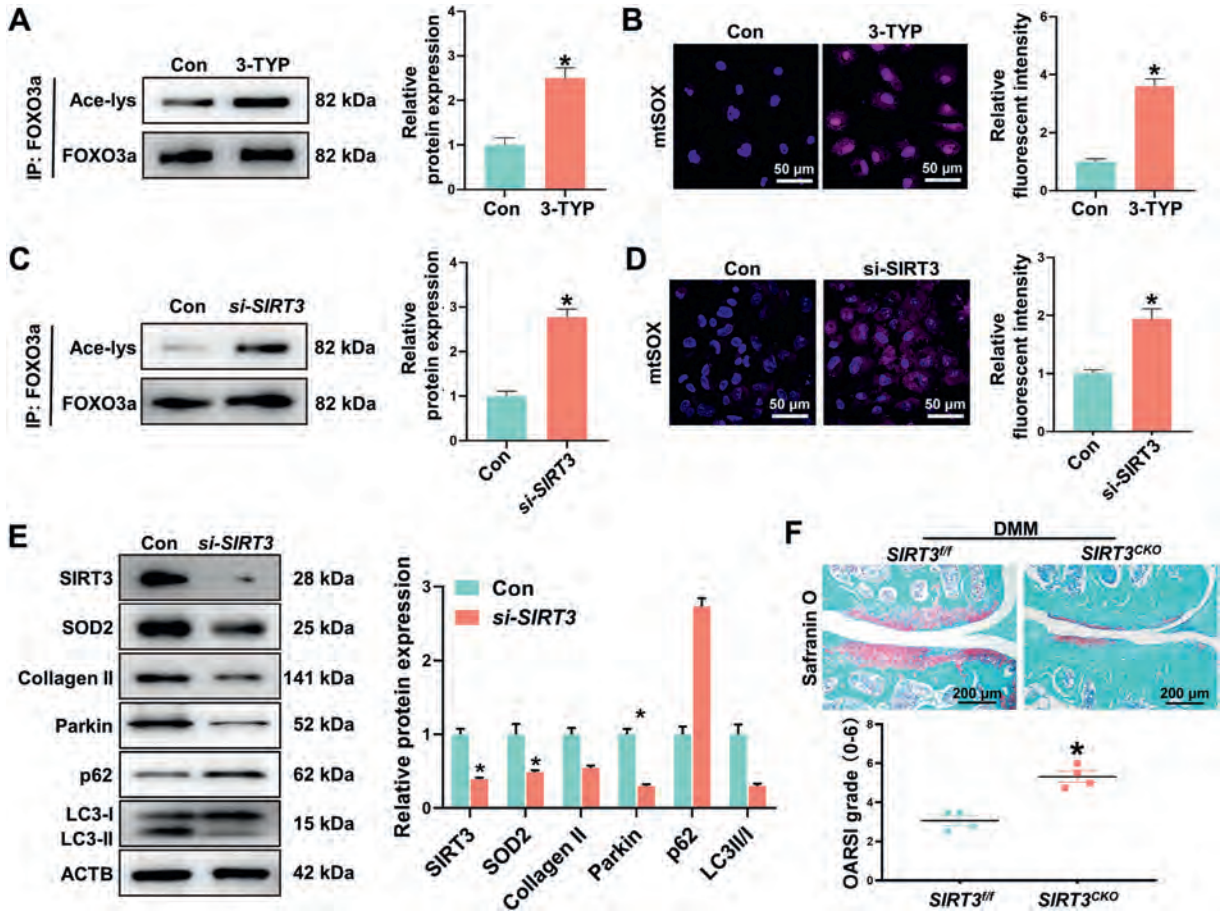

Figure 6 SIRT3 knockdown in chondrocytes promotes FOXO3a acetylation and aggravates the progression of OA. (A) Western blot analysis of the acetylation of FOXO3a in C28/I2 cells treated with or without 3-TYP. $n = 3$, $^*P < 0.05$. (B) The detection and analysis of mtSOX expression in C28/I2 cells treated with or without 3-TYP. $n = 3$, $^*P < 0.05$. (C) Western blot analysis of the acetylation of FOXO3a in C28/I2 cells transfected with or without *SIRT3 siRNA* (*si-SIRT3*). $n = 3$, $^*P < 0.05$. (D) The detection and analysis of mtSOX expression in C28/I2 cells transfected with or without *si-SIRT3*. $n = 3$, $^*P < 0.05$. (E) Western blot analysis of the expression of SIRT3, SOD2, Collagen II, Parkin, p62, and LC3 in C28/I2 cells transfected with or without *si-SIRT3*. $n = 3$, $^*P < 0.05$. (F) The representative safranin O staining images and analytical results with the Osteoarthritis Research Society International (OARSI) scoring system of the knee joints from $SIRT3^{f/f}$ and $SIRT3^{CKO}$ mice that underwent DMM surgery. $n = 6$, $^*P < 0.05$. All data are presented as the mean ± SEM. A paired *t*-test was used for statistical analysis.

the protein acetylation was profoundly enhanced in the cartilage of $SIRT3^{cKO}$ mice, along with decreased expression of SOD2 and Collagen II (Fig. S6B and S6C). Next, the $SIRT3^{flox/flox}$ and $SIRT3^{cKO}$ mice were further subjected to post-traumatic OA using classical destabilization of the medial meniscus (DMM) surgery. OA development was significantly accelerated in $SIRT3^{cKO}$ mice as compared with $SIRT3^{flox/flox}$ mice (Fig. 6F). Taken together, our results demonstrated that inhibition of SIRT3 could suppress mitophagy and induce mitochondrial dysfunction *via* enhancing the acetylation of FOXO3a in chondrocytes, which subsequently resulted in aggravated cartilage degradation.

3.7. Overexpression of SIRT3 suppresses ROS and protects chondrocytes from CRTAC1-induced degradation

To further demonstrate whether decreased SIRT3 is responsible for CRTAC1-induced chondrocyte degradation, we conducted rescue experiments with the transfection of *LV-SIRT3*. Overexpression of SIRT3 in CRTAC1-treated chondrocytes increased the expression of COL2A1 to near normal levels, and effectively attenuated MMP13 expression and ROS levels (Fig. 7A–C). Next, we sought to investigate whether restoration of SIRT3 could attenuate the progression of OA *in vivo*. 10 μL of *AAV-SIRT3* (1×10^{11} particles) or negative control was injected into the knee joint every two weeks after DMM. Intra-articular injection of *AAV-SIRT3* restored SIRT3 expression and suppressed protein acetylation in the cartilage of OA mice (Fig. 7D–F). Assessing by safranin O-fast green and IHC staining, we observed that overexpression of SIRT3 substantially inhibited articular cartilage erosion, and rescued Collagen II compared to OA mice injected with *AAV-NC* (Fig. 7G and H). The OARSI scores also suggested *AAV-SIRT3*-treated knee joints exhibited a milder OA phenotype (Fig. 7H), which revealed a therapeutic effect of SIRT3 for treating cartilage degeneration in OA progression.

3.8. CRTAC1 suppresses SIRT3 transcription via regulating NRF2

To explore the mechanism of CRTAC1-mediated suppression of SIRT3 in chondrocytes, we found that the binding of NRF2, a

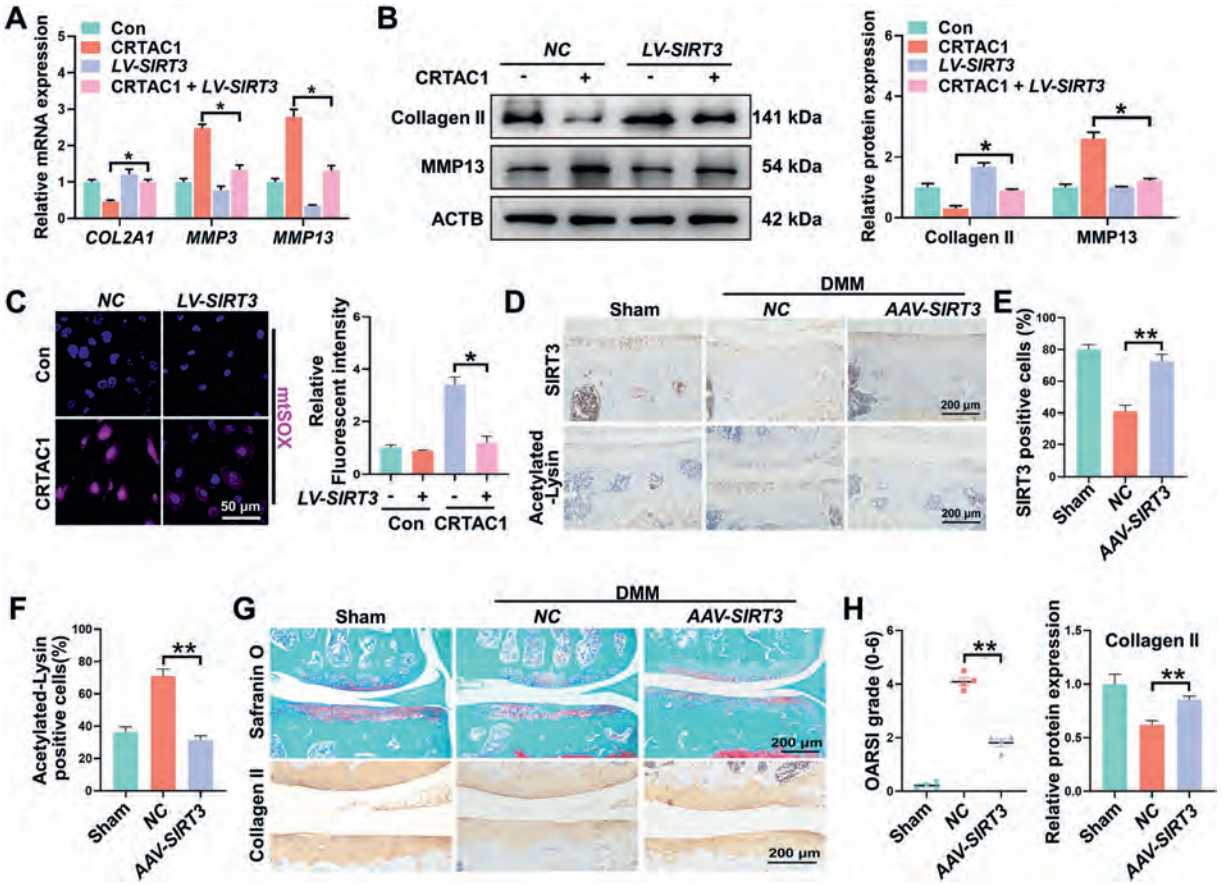

Figure 7 Overexpression of SIRT3 suppresses ROS and protects chondrocytes from CRTAC1-induced degradation. (A) qPCR analysis of the expression of *COL2A1*, *MMP3* and *MMP13* in recombinant CRTAC1-treated C28/I2 cells transfected with or without *LV-SIRT3*. $n = 3$, $^{*}P < 0.05$. (B) Western blot analysis of the expression of Collagen II and MMP13 in recombinant CRTAC1-treated C28/I2 cells transfected with or without *LV-SIRT3*. $n = 3$, $^{*}P < 0.05$. (C) The detection and analysis of mtSOX expression in recombinant CRTAC1-treated C28/I2 cells transfected with or without *LV-SIRT3*. $n = 3$, $^{*}P < 0.05$. (D−F) The representative images and analysis of immunohistochemistry staining of SIRT3 and acetylated-lysine in cartilage from DMM mice injected with or without *AAV-SIRT3*. $n = 6$, $^{**}P < 0.01$. (G, H) The representative images and analysis of safranin O staining and Collagen II staining for knee joints from DMM mice injected with or without *AAV-SIRT3*. $n = 6$, $^{**}P < 0.01$. All data are presented as the mean ± SEM. One-way ANOVA with Tukey's *post hoc* test was used for statistical analysis.

positive regulator of SIRT3, on the promoter region of SIRT3 was significantly impaired by CRTAC1 treatment (Fig. 8A). The immunofluorescence and immunoblot results also determined that CRTAC1 impaired the nuclear translocation of NRF2 (Fig. 8B, Supporting Information Fig. S7). Activation of NRF2 by tBHQ could effectively compromise CRTAC1-mediated reduction of SIRT3 (Fig. 8B−D, Supporting Information Fig. S8A). Interestingly, we found that the mRNA levels of NRF2 were not changed in CRTAC1-treated C28/I2 cells (Fig. S8B), which indicated that CRTAC1-mediated reduction of NRF2 was not due to its transcription. Molecular docking was performed, and the predicted binding mode revealed a good shape match between CRTAC1 and NRF2 (Fig. 8E). As shown in Fig. 8F, the results of immunofluorescent staining revealed that exogenous CRTAC1 could be uptake by C28/I2 cells and co-localized with NRF2 *in vitro*. The interaction between CRTAC1 and NRF2 was further determined by coimmunoprecipitation assay, which showed that CRTAC1 physically interacted with endogenous NRF2 in C28/I2 cells (Fig. 8G). These results suggested that CRTAC1 could interact with NRF2 and impair the nuclear translocation of NRF2, which resulted in suppressed transcription of SIRT3 in chondrocytes.

4. Discussion

OA is the most common type of joint disease, characterized by the degeneration of cartilage. As OA progresses, it can lead to disability among older adults, resulting in socioeconomic consequences[34]. The etiology of OA is complex and involves multiple factors, including mechanical stresses placed on the joints and predisposing factors such as aging[35]. In this study, we demonstrated that CRTAC1 was highly expressed in senescent FLS, which was found to be a crucial regulator in cartilage degradation *via* using both loss- and gain-of-function models. In addition, it was documented that the plasma CRTAC1 levels were tightly associated with OA diagnosis, which was the best predictor of OA progression to joint replacement[11]. The present study demonstrated that CRTAC1-mediated mitophagy suppression and mitochondrial damage existed in the chondrocytes and contributed to the chondrocyte degradation in a FOXO3a-dependent manner. It was documented that the alterations in the structure, dynamics, and genome stability of mitochondria would lead to decreased mitochondrial respiration and an excessive production of ROS, ultimately resulting in oxidative damage, which serves as a

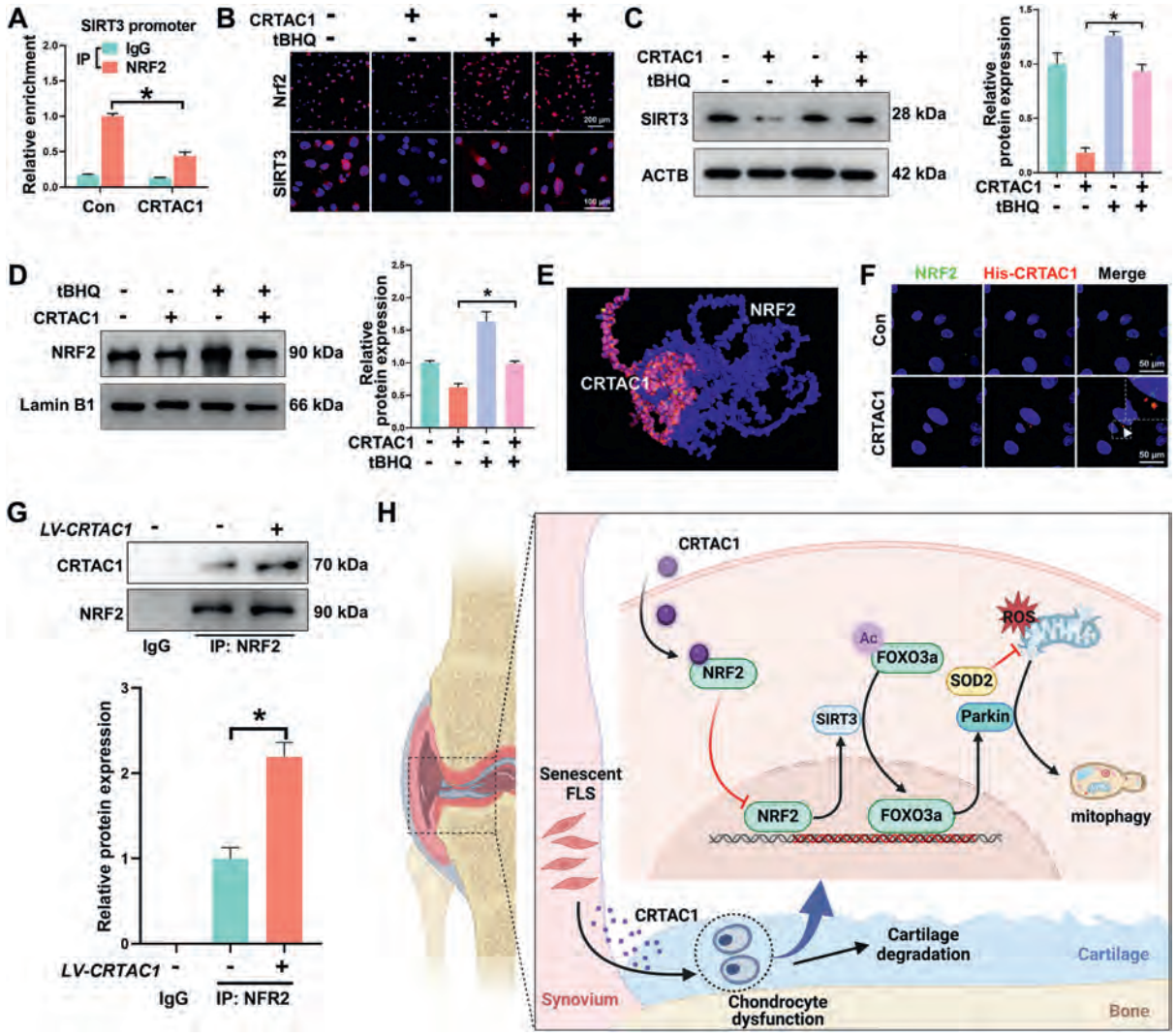

Figure 8 CRTAC1 suppresses SIRT3 transcription *via* regulating NRF2. (A) ChIP assay of NRF2 binding to the promoter of SIRT3 in C28/I2 cells treated with or without recombinant CRTAC1. $n = 3$, $^*P < 0.05$. (B) Immunofluorescence staining of NRF2 and SIRT3 in recombinant CRTAC1-treated C28/I2 cells, accompanied with or without tBHQ treatment. (C, D) Western blot analysis of the expression of SIRT3 and NRF2 in recombinant CRTAC1-treated C28/I2 cells, accompanied with or without tBHQ treatment. $n = 3$, $^*P < 0.05$. (E) The molecular docking simulation of CRTAC1 and NRF2. (F) Representative images of coimmunostaining of NRF2 and His-CRTAC1 in C28/I2 cells treated with or without recombinant CRTAC1. (G) Co-IP assay of the binding between NRF2 and CRTAC1 in C28/I2 cells transfected with or without *LV-CRTAC1*. $n = 3$, $^*P < 0.05$. (H) Schematic representation of mechanisms by which senescent FLS-derived CRTAC1 mediates cartilage degradation in OA progression. All data are presented as the mean ± SEM. Paired *t*-test (A) and one-way ANOVA with Tukey's *post hoc* test (C, D, G) were used for statistical analysis.

hallmark of OA[36]. The expression of ROS is typically low in normal chondrocytes, which becomes elevated in OA progression[37]. Currently, impairing ROS production in the mitochondria is considered a novel approach to modify the development of OA[38].

FOXO3a, as an important member of the FOXO family, displayed a definite antioxidant stress effect *via* inducing the expression of SOD2[39,40]. SOD2 could further scavenge ROS by converting the superoxide anion radical into hydrogen peroxide and molecular oxygen, thus maintaining redox homeostasis. SOD2 knockout mice exhibited increased cartilage degeneration during aging[41]. The function of FOXO3a is crucially regulated through phosphorylation, which keeps it inactive in the cytoplasm as a phosphorylated form, and transfers to the nucleus to activate target genes after dephosphorylation[42]. Very recently, growing evidence has demonstrated that the SIRT3/FOXO3a axis serves as a critical contributor to mitochondrial protection in response to cellular stresses[16,43]. SIRT3 is a mitochondrial deacetylase involved in several important metabolic processes[44]. The deacetylation of FOXO3a by SIRT3 also decreases the phosphorylation of FOXO3a[45]. In our work, SIRT3 was found to be a critical regulator in CRTAC1-induced mitochondrial dysfunction. It physically modulated the deacetylation of FOXO3a, which ultimately promoted the transcription activity of FOXO3a. Whole-body knockout of SIRT3 could accelerate the progression of OA[17]. In this study, we further proved that conditional knockout of SIRT3 in the cartilage could aggravate the development of OA. Overexpression of SIRT3 could inhibit the degeneration of

cartilage in OA mouse models. *In vitro*, CRTAC1 could decrease the expression of SIRT3 in chondrocytes. However, the role of CRTAC1 in regulating SIRT3 expression has not been fully elucidated.

NRF2 modulates the transcription of various genes involved in antioxidant defense and cell protection, which are essential for combating oxidative stress[46]. There is compelling evidence of a close relationship between NRF2 and SIRT3, as NRF2 binds to the SIRT3 promoter and regulates its transcription[47]. Studies have shown that NRF2 could protect hepatocytes from endoplasmic reticulum stress-induced liver injury by increasing SIRT3 expression[48]. Inhibition of NRF2 leads to a remarkable reduction in SIRT3 expression, accompanied by enhanced acetylation of FOXO3a[49]. *In vitro*, we demonstrated that CRTAC1 impaired the binding ability of NRF2 on the promoter region of SIRT3 in chondrocytes. In addition, CRTAC1 physically interacted with NRF2, resulting in suppressed nuclear translocation of NRF2 in chondrocytes. Under normal conditions, when normal cells are exposed to external stimuli, the NRF2 protein dissociates from the Keap1 protein and binds with antioxidant response elements (ARE) to form the NRF2−ARE complex. The NRF2−ARE complex is then transported to the nucleus, where it regulates the transcription of multiple genes responsible for antioxidant defense and cellular protection[50]. Activation of NRF2 by tBHQ could effectively elevate the nuclear translocation of NRF2 and compromise CRTAC1-mediated reduction of SIRT3.

5. Conclusions

In summary, our findings significantly expand the understanding of how senescent FLS secrete CRTAC1 to promote chondrocyte degeneration and OA progression. For the first time, we provide evidence that CRTAC1 induces mitochondrial dysfunction by modulating FOXO3a in a NRF2−SIRT3-dependent manner (Fig. 8H). Our study underscores the critical role of SIRT3-mediated deacetylation in chondrocyte degeneration, offering novel insights into the molecular mechanisms through which CRTAC1 influences OA progression. These findings also highlight potential therapeutic strategies targeting this pathway for the treatment of OA.

Acknowledgements

This work was supported by research grants from the National Major Research plan of NSFC (92368201); National Natural Science Foundation of China (82272530 and 82372459); Jiangsu Province Medical Innovation Center of Orthopedic Surgery (CXZX202214, China). China Postdoctoral Science Foundation (2024T170409); Excellent Postdoctoral Program of Jiangsu Province (2022ZB688, China); Youth Thousand Talents Program of China (13004001); The Research Team Start-up Funds of Nanjing University (14912203, China).

Author contributions

Xiang Chen: Writing−original draft, Methodology, Investigation, Data curation, Funding acquisition. Wang Gong: Formal analysis, Data curation, investigation. Pan Zhang: Investigation. Chengzhi Wang: Investigation. Bin Liu: Investigation. Xiaoyan Shao: Investigation. Yi He: Investigation. Na Liu: Investigation. Jiaquan Lin: Investigation. Jianghui Qin: Resources, Funding acquisition. Qing Jiang: Supervision, Resources, Project administration, Funding acquisition, Conceptualization. Baosheng Guo: Visualization, Validation, Supervision, Resources, Project administration, Funding acquisition, Conceptualization.

Conflicts of interest

The authors declare no competing interests.

Appendix A. Supporting information

Supporting information to this article can be found online at https://doi.org/10.1016/j.apsb.2025.08.014.

References

1. Edwards JJ, Khanna M, Jordan KP, Jordan JL, Bedson J, Dziedzic KS. Quality indicators for the primary care of osteoarthritis: a systematic review. *Ann Rheum Dis* 2015;**74**:490−8.
2. Martin JA, Brown TD, Heiner AD, Buckwalter JA. Chondrocyte senescence, joint loading and osteoarthritis. *Clin Orthop Relat Res* 2004;**427**(Suppl):S96−103.
3. Jeon OH, David N, Campisi J, Elisseeff JH. Senescent cells and osteoarthritis: a painful connection. *J Clin Investig* 2018;**128**: 1229−37.
4. Chen X, Gong W, Shao X, Shi T, Zhang L, Dong J, et al. METTL3-mediated m(6)A modification of ATG7 regulates autophagy−GATA4 axis to promote cellular senescence and osteoarthritis progression. *Ann Rheum Dis* 2022;**81**:87−99.
5. Jiang Y, Tuan RS. Origin and function of cartilage stem/progenitor cells in osteoarthritis. *Nat Rev Rheumatol* 2015;**11**:206−12.
6. Hui AY, McCarty WJ, Masuda K, Firestein GS, Sah RL. A systems biology approach to synovial joint lubrication in health, injury, and disease. *Wiley Interdiscip Rev Syst Biol Med* 2012;**4**:15−37.
7. Ritter SY, Subbaiah R, Bebek G, Crish J, Scanzello CR, Krastins B, et al. Proteomic analysis of synovial fluid from the osteoarthritic knee: comparison with transcriptome analyses of joint tissues. *Arthritis Rheum* 2013;**65**:981−92.
8. Wang Q, Rozelle AL, Lepus CM, Scanzello CR, Song JJ, Larsen DM, et al. Identification of a central role for complement in osteoarthritis. *Nat Med* 2011;**17**:1674−9.
9. Steck E, Benz K, Lorenz H, Loew M, Gress T, Richter W. Chondrocyte expressed protein-68 (CEP-68), a novel human marker gene for cultured chondrocytes. *Biochem J* 2001;**353**:169−74.
10. Steck E, Bräun J, Pelttari K, Kadel S, Kalbacher H, Richter W. Chondrocyte secreted CRTAC1: a glycosylated extracellular matrix molecule of human articular cartilage. *Matrix Biol* 2007;**26**:30−41.
11. Styrkarsdottir U, Lund SH, Saevarsdottir S, Magnusson MI, Gunnarsdottir K, Norddahl GL, et al. The CRTAC1 protein in plasma is associated with osteoarthritis and predicts progression to joint replacement: a large-scale proteomics scan in Iceland. *Arthritis Rheumatol* 2021;**73**:2025−34.
12. Szilagyi IA, Vallerga CL, Boer CG, Schiphof D, Ikram MA, Bierma-Zeinstra SMA, et al. Plasma proteomics identifies CRTAC1 as a biomarker for osteoarthritis severity and progression. *Rheumatology* 2023;**62**:1286−95.
13. Ge X, Ritter SY, Tsang K, Shi R, Takei K, Aliprantis AO. Sex-specific protection of osteoarthritis by deleting cartilage acid protein 1. *PLoS One* 2016;**11**:e0159157.
14. Blanco FJ, June RK. 2nd. Cartilage metabolism, mitochondria, and osteoarthritis. *J Am Acad Orthop Surg* 2020;**28**:e242−4.
15. Qiao L, Li Z, Li B, Zhang F, Yao Z, Wu C, et al. Combination of anti-inflammatory therapy and RNA interference by light-inducible hybrid nanomedicine for osteoarthritis treatment. *Acta Pharm Sin B* 2024;**14**: 5008−25.

16. Tseng AH, Shieh SS, Wang DL. SIRT3 deacetylates FOXO3 to protect mitochondria against oxidative damage. *Free Radic Biol Med* 2013;**63**: 222−34.
17. Fu Y, Kinter M, Hudson J, Humphries KM, Lane RS, White JR, et al. Aging promotes sirtuin 3-dependent cartilage superoxide dismutase 2 acetylation and osteoarthritis. *Arthritis Rheumatol* 2016;**68**:1887−98.
18. Charan J, Kantharia ND. How to calculate sample size in animal studies?. *J Pharmacol Pharmacother* 2013;**4**:303−6.
19. Pritzker KP, Gay S, Jimenez SA, Ostergaard K, Pelletier JP, Revell PA, et al. Osteoarthritis cartilage histopathology: grading and staging. *Osteoarthr Cartil* 2006;**14**:13−29.
20. Goldring MB, Birkhead JR, Suen LF, Yamin R, Mizuno S, Glowacki J, et al. Interleukin-1 beta-modulated gene expression in immortalized human chondrocytes. *J Clin Investig* 1994;**94**:2307−16.
21. Stuart T, Butler A, Hoffman P, Hafemeister C, Papalexi E, Mauck 3rd WM, et al. Comprehensive integration of single-cell data. *Cell* 2019;**177**:1888.
22. Chang J, Wang Y, Shao L, Laberge RM, Demaria M, Campisi J, et al. Clearance of senescent cells by ABT263 rejuvenates aged hematopoietic stem cells in mice. *Nat Med* 2016;**22**:78−83.
23. Baker DJ, Wijshake T, Tchkonia T, LeBrasseur NK, Childs BG, van de Sluis B, et al. Clearance of p16Ink4a-positive senescent cells delays ageing-associated disorders. *Nature* 2011;**479**:232−6.
24. Kang L, Xiang Q, Zhan S, Song Y, Wang K, Zhao K, et al. Restoration of autophagic flux rescues oxidative damage and mitochondrial dysfunction to protect against intervertebral disc degeneration. *Oxid Med Cell Longev* 2019;**2019**:7810320.
25. Liu Y, Ao X, Ding W, Ponnusamy M, Wu W, Hao X, et al. Critical role of FOXO3a in carcinogenesis. *Mol Cancer* 2018;**17**:104.
26. Bolduc JA, Collins JA, Loeser RF. Reactive oxygen species, aging and articular cartilage homeostasis. *Free Radic Biol Med* 2019;**132**:73−82.
27. Ruankham W, Suwanjang W, Phopin K, Songtawee N, Prachayasittikul V, Prachayasittikul S. Modulatory effects of alpha-mangostin mediated by SIRT1/3-FOXO3a pathway in oxidative stress-induced neuronal cells. *Front Nutr* 2021;**8**:714463.
28. Chen M, Liu Y, Liu Q, Deng S, Liu Y, Chen J, et al. Nanoengineered cargo with targeted *in vivo Foxo3* gene editing modulated mitophagy of chondrocytes to alleviate osteoarthritis. *Acta Pharm Sin B* 2025;**15**:571−91.
29. Fasano C, Disciglio V, Bertora S, Lepore Signorile M, Simone C. FOXO3a from the nucleus to the mitochondria: a round trip in cellular stress response. *Cells* 2019;**8**:1110.
30. Brunet A, Sweeney LB, Sturgill JF, Chua KF, Greer PL, Lin Y, et al. Stress-dependent regulation of FOXO transcription factors by the SIRT1 deacetylase. *Science* 2004;**303**:2011−5.
31. Zhang P, Tu B, Wang H, Cao Z, Tang M, Zhang C, et al. Tumor suppressor p53 cooperates with SIRT6 to regulate gluconeogenesis by promoting FoxO1 nuclear exclusion. *Proc Natl Acad Sci U S A* 2014; **111**:10684−9.
32. Sundaresan NR, Gupta M, Kim G, Rajamohan SB, Isbatan A, Gupta MP. Sirt3 blocks the cardiac hypertrophic response by augmenting Foxo3a-dependent antioxidant defense mechanisms in mice. *J Clin Investig* 2009;**119**:2758−71.
33. Kim HS, Patel K, Muldoon-Jacobs K, Bisht KS, Aykin-Burns N, Pennington JD, et al. SIRT3 is a mitochondria-localized tumor suppressor required for maintenance of mitochondrial integrity and metabolism during stress. *Cancer Cell* 2010;**17**:41−52.
34. Emery CA, Whittaker JL, Mahmoudian A, Lohmander LS, Roos EM, Bennell KL, et al. Establishing outcome measures in early knee osteoarthritis. *Nat Rev Rheumatol* 2019;**15**:438−48.
35. Loeser RF, Collins JA, Diekman BO. Ageing and the pathogenesis of osteoarthritis. *Nat Rev Rheumatol* 2016;**12**:412−20.
36. Mobasheri A, Rayman MP, Gualillo O, Sellam J, van der Kraan P, Fearon U. The role of metabolism in the pathogenesis of osteoarthritis. *Nat Rev Rheumatol* 2017;**13**:302−11.
37. Altay MA, Ertürk C, Bilge A, Yaptı M, Levent A, Aksoy N. Evaluation of prolidase activity and oxidative status in patients with knee osteoarthritis: relationships with radiographic severity and clinical parameters. *Rheumatol Int* 2015;**35**:1725−31.
38. Wang J, Wang K, Huang C, Lin D, Zhou Y, Wu Y, et al. SIRT3 activation by dihydromyricetin suppresses chondrocytes degeneration *via* maintaining mitochondrial homeostasis. *Int J Biol Sci* 2018;**14**: 1873−82.
39. Ferber EC, Peck B, Delpuech O, Bell GP, East P, Schulze A. FOXO3a regulates reactive oxygen metabolism by inhibiting mitochondrial gene expression. *Cell Death Differ* 2012;**19**:968−79.
40. Kops GJ, Dansen TB, Polderman PE, Saarloos I, Wirtz KW, Coffer PJ, et al. Forkhead transcription factor FOXO3a protects quiescent cells from oxidative stress. *Nature* 2002;**419**:316−21.
41. Scott JL, Gabrielides C, Davidson RK, Swingler TE, Clark IM, Wallis GA, et al. Superoxide dismutase downregulation in osteoarthritis progression and end-stage disease. *Ann Rheum Dis* 2010;**69**: 1502−10.
42. Nho RS, Hergert P. FoxO3a and disease progression. *World J Biol Chem* 2014;**5**:346−54.
43. Guo L, Xiang W, Pan Z, Gu H, Jiang X. Post-translational modifications of collagen and its related diseases in metabolic pathways. *Acta Pharm Sin B* 2025;**15**:1773−95.
44. Zhu J, Yang Q, Li H, Wang Y, Jiang Y, Wang H, et al. Sirt3 deficiency accelerates ovarian senescence without affecting spermatogenesis in aging mice. *Free Radic Biol Med* 2022;**193**:511−25.
45. Tseng AH, Wu LH, Shieh SS, Wang DL. SIRT3 interactions with FOXO3 acetylation, phosphorylation and ubiquitinylation mediate endothelial cell responses to hypoxia. *Biochem J* 2014;**464**: 157−68.
46. Ma Q. Role of nrf2 in oxidative stress and toxicity. *Annu Rev Pharmacol Toxicol* 2013;**53**:401−26.
47. Oh JY, Choi GE, Lee HJ, Jung YH, Chae CW, Kim JS, et al. 17β-Estradiol protects mesenchymal stem cells against high glucose-induced mitochondrial oxidants production *via* Nrf2/Sirt3/MnSOD signaling. *Free Radic Biol Med* 2019;**130**:328−42.
48. Kim A, Koo JH, Lee JM, Joo MS, Kim TH, Kim H, et al. NRF2-mediated SIRT3 induction protects hepatocytes from ER stress-induced liver injury. *FASEB J* 2022;**36**:e22170.
49. Zhang B, Yang J, Li X, Zhu H, Sun J, Jiang L, et al. Tetrahydrocurcumin ameliorates postinfarction cardiac dysfunction and remodeling by inhibiting oxidative stress and preserving mitochondrial function *via* SIRT3 signaling pathway. *Phytomedicine* 2023;**121**: 155127.
50. Periyasamy P, Shinohara T. Age-related cataracts: role of unfolded protein response, Ca^{2+} mobilization, epigenetic DNA modifications, and loss of Nrf2/Keap1 dependent cytoprotection. *Prog Retin Eye Res* 2017;**60**:1−19.